European Journal of Medicinal Chemistry 87 (2014) 519–528

Contents lists available at ScienceDirect

European Journal of Medicinal Chemistry

journal homepage: http://www.elsevier.com/locate/ejmech

Original article

Selection of an optimal cysteine-containing peptide-based chelator for labeling of affibody molecules with ^{188}Re

Mohamed Altai [a], Hadis Honarvar [a], Helena Wållberg [b, c], Joanna Strand [a], Zohreh Varasteh [d], Maria Rosestedt [d], Anna Orlova [d], Finn Dunås [e], Mattias Sandström [f], John Löfblom [b], Vladimir Tolmachev [a, *], Stefan Ståhl [b]

[a] Division of Biomedical Radiation Sciences, Rudbeck Laboratory, Uppsala University, Uppsala, Sweden
[b] KTH Royal Institute of Technology, School of Biotechnology, Division of Protein Technology, Stockholm, Sweden
[c] Division of Biochemistry, Dept. of Medical Biochemistry and Biophysics, Karolinska Institutet, Stockholm, Sweden
[d] Preclinical PET Platform, Department of Medicinal Chemistry, Uppsala University, Uppsala, Sweden
[e] Affibody AB, Stockholm, Sweden
[f] Medical Physics Uppsala University Hospital, Uppsala, Sweden

ARTICLE INFO

Article history:
Received 1 April 2014
Received in revised form
23 September 2014
Accepted 25 September 2014
Available online 26 September 2014

Keywords:
Rhenium-188
Affibody
HER2
Peptide-based chelator
Biodistribution
Radionuclide therapy

ABSTRACT

Affibody molecules constitute a class of small (7 kDa) scaffold proteins that can be engineered to have excellent tumor targeting properties. High reabsorption in kidneys complicates development of affibody molecules for radionuclide therapy. In this study, we evaluated the influence of the composition of cysteine-containing C-terminal peptide-based chelators on the biodistribution and renal retention of ^{188}Re-labeled anti-HER2 affibody molecules. Biodistribution of affibody molecules containing GGXC or GXGC peptide chelators (where X is G, S, E or K) was compared with biodistribution of a parental affibody molecule $Z_{HER2:2395}$ having a KVDC peptide chelator. All constructs retained low picomolar affinity to HER2-expressing cells after labeling. The biodistribution of all ^{188}Re-labeled affibody molecules was in general comparable, with the main observed difference found in the uptake and retention of radioactivity in excretory organs. The ^{188}Re-$Z_{HER2:V2}$ affibody molecule with a GGGC chelator provided the lowest uptake in all organs and tissues. The renal retention of ^{188}Re-$Z_{HER2:V2}$ (3.1 ± 0.5 %ID/g at 4 h after injection) was 55-fold lower than retention of the parental ^{188}Re-$Z_{HER2:2395}$ (172 ± 32 %ID/g). We show that engineering of cysteine-containing peptide-based chelators can be used for significant improvement of biodistribution of ^{188}Re-labeled scaffold proteins, particularly reduction of their uptake in excretory organs.

1. Introduction

The use of monoclonal antibodies against cancer-associated antigens improves survival of patients with disseminated cancer. However, a substantial fraction of tumors show primary drug resistance. Development of a secondary (acquired) resistance has also been identified during the course of targeted therapy despite preserved antigen expression [1–5]. Targeted radionuclide therapy is a promising method for treatment of both inoperable primary and disseminated antibody-resistant tumors. Several classes of radiolabeled proteins have been used for delivery of radionuclides to tumors *in vivo*, utilizing the specific binding of these agents to phenotypic molecular alterations in malignant cells. In fact, tumor targeting with radiolabeled antibodies for detection of malignancy or for therapeutic purposes has been reported as early as the 1950's [6,7]. However, both preclinical and clinical investigations have revealed that the clinical effect of radioimmunotherapy (RIT) on bulky solid tumors is limited [8]. Due to their large size (150 kDa), radiolabeled intact antibodies are characterized by slow clearance from blood and poor tumor penetration [8]. Several alternative methods have been developed to overcome problems associated with conventional RIT. The use of smaller enzymatically produced antibody fragments [8,9], analogues of naturally existing peptide ligands to receptors overexpressed in tumors [10], and pretargeting strategies [11] constitute examples of new approaches aiming to deliver radionuclides to tumors while sparing healthy tissues. Another promising approach for the development of high affinity

* Corresponding author. Unit of Biomedical Radiation Sciences, Rudbeck Laboratory, Uppsala University, SE-751 85 Uppsala, Sweden.
E-mail address: vladimir.tolmachev@bms.uu.se (V. Tolmachev).

http://dx.doi.org/10.1016/j.ejmech.2014.09.082

small-size agents for targeted radionuclide therapy is the use of engineered scaffold proteins.

Affibody molecules were one of the first evaluated classes of non-immunoglobulin scaffold proteins for *in vivo* radionuclide targeting. These high affinity ligands are based on a 58 amino acid (7 kDa) triple α-helical scaffold derived from domain B of staphylococcal protein A [12,13]. Thirteen surface located amino acids on helices 1 and 2 have been randomized, generating large combinatorial libraries from which affibody variants targeting the desired antigen could be selected. Due to their generally high affinity towards specific molecular targets and their small size, affibody molecules are attractive candidates for tumor-targeting applications [14]. An important feature is the robustness of this targeting protein. Affibody molecules typically tolerate the denaturation during labeling procedures (e.g. exposure to high temperature or lipophilic solvents), since they rapidly and completely refold to their initial structure after returning to physiological conditions [15]. This characteristic permits labeling in a pH range from 3.6 [16] to 11.0 [17] and at temperatures up to 90 °C [18], without losing binding capacity. This allows labeling with a large variety of nuclides and enables to select an optimal one for each particular application. An anti-Human Epidermal Growth Factor Receptor type 2 (HER2) affibody molecule has been extensively investigated, primarily for tumor imaging application. This affibody molecule binds with picomolar affinity (22 pM) to the extracellular domain of HER2 receptors [19].

Cellular processing studies have shown that internalization of anti-HER2 affibody molecules is relatively slow [20]. Typically, less than 30% of the bound tracer was internalized after 24 h. Therefore, the use of a residualizing radiometal label to increase radioactivity retention in tumor cells is of less importance for the anti-HER2 affibody molecule, because most of the retained activity is membrane bound. However, similar to other small proteins and peptides, efficient tumor targeting was associated with significant renal accumulation of affibody molecules labeled with residualizing radiometals such as ^{177}Lu, ^{90}Y, and ^{114m}In [21–23]. This accumulation is attributed to extensive tubular reabsorption after glomerular filtration [24].

A high level of reabsorption exposes the kidneys to irradiation at high doses, which would potentially compromise their functionality. An approach to reduce this high renal dose is fusing affibody molecules to a 46 amino acid albumin binding domain (ABD), derived from streptococcal protein G. The non-covalent binding of such affibody-ABD fusion proteins to albumin *in vivo* was found to prolong circulation times and reduce kidney accumulation [21,25]. However, long residence time of the conjugate in circulation may result in higher irradiation of the very radiosensitive bone marrow. On the contrary, affibody molecules labeled with non-residualizing labels provide rapid clearance of radioactivity from kidneys without reducing tumor dose while avoiding long circulation times [26].

Earlier, a series of studies involving labeling of affibody molecules with technetium-99m (^{99m}Tc) using peptide-based N_3S chelators has been performed (for reviews concerning labeling with technetium and rhenium radioisotopes, see Refs. [27–29]). These studies demonstrated that targeting properties of labeled probes can be improved by selecting an optimal chelator [30–36]. Substitution of the amino acids forming the chelator for binding ^{99m}Tc had a profound effect on the biodistribution profile of affibody molecules. Initially, the ^{99m}Tc-labeling of affibody molecules was performed using the mercaptoacetyl-glycyl-glycyl-glycyl (maGGG) chelator coupled to the N-terminus of the anti-HER2 affibody molecule $Z_{HER2:342}$ [37]. The tracer was capable of targeting HER2 *in vivo*, but underwent high hepatobiliary excretion. Combination of serine (polar) and glutamic acid (charged) in mercaptoacetyl-containing chelators (maESE) provided a radiolabeled conjugate with less hepatobiliary excretion and renal retention of radioactivity [38]. To permit recombinant production, cysteine as the thiol-bearing moiety was introduced on the C-terminus of the anti-HER2 affibody molecule. The tracer ^{99m}Tc-$Z_{HER2:2395}$-Cys (having KVDC sequence at the C-terminus) demonstrated excellent biodistribution except from an elevated kidney uptake [34]. To reduce the renal uptake, a GSEC chelator (a "mirror" C-terminal homolog of maESE-) was designed [33]. The use of GSEC resulted in four-fold reduction of renal retention in comparison with KVDC. For further optimization of cysteine containing peptide-based chelators, a series of recombinantly produced derivatives containing GSEC, GGGC, GGSC, GGEC, or GGKC peptide chelators at the C-terminus (designated as $Z_{HER2:V1}$, $Z_{HER2:V2}$, $Z_{HER2:V3}$, $Z_{HER2:V4}$ and $Z_{HER2:V5}$ respectively) was generated [35]. The *in vivo* evaluation of the ^{99m}Tc-labeled variants demonstrated low hepatobiliary excretion and rapid blood clearance. The renal retention varied considerably, with the GGGC containing anti-HER2 affibody molecule showing the lowest kidney associated radioactivity (6.4 ± 0.6% ID/g at 4 h p.i.). Further optimization showed that the order of amino acids in the chelating sequence influenced renal uptake of some conjugates at 1 h after injection, but the difference decreased at later time points [36]. The results obtained with ^{99m}Tc-labeled anti-HER2 affibody molecules prompted us to utilize this experience in developing an affibody-based tumor-targeting agent for peptide-based radionuclide therapy.

Rhenium is a chemical analogue of technetium, and two rhenium isotopes, ^{186}Re ($T_{½}$ = 3.72 days; $E_{\bar{\beta}}$max = 1.08 MeV) and ^{188}Re ($T_{½}$ = 17.0 h; $E_{\bar{\beta}}$ max = 2.1 MeV), are considered suitable for therapy. High-energy (^{188}Re) or medium energy (^{186}Re) β-particles are well suited for eradication of both bulky non-operable tumors and large metastases. The γ-radiation of these nuclides (^{186}Re: Eγ = 155 keV,15%; ^{188}Re: Eγ = 137 keV, 9%) enables *in vivo* imaging of the biodistribution of rhenium-labeled conjugates, which could be used for patient-specific dosimetry. At the same time, the γ-radiation would not contribute too much to the whole-body irradiation due to low abundance. The half-life of ^{188}Re matches better the rapid *in vivo* kinetics of affibody molecules. In addition, ^{188}Re is produced using a ^{188}W/^{188}Re generator, which reduces the radionuclide costs and facilitates the logistics of therapy. Furthermore, this nuclide might be produced in a no-carrier-added state, with a high specific radioactivity. Thus ^{188}Re is an attractive label for affibody-based radionuclide therapy on the precondition that the issue of renal accumulation is solved. Rhenium isotopes (mainly ^{188}Re) have been used for RIT to eliminate large burdens of leukemia in conjunction with standard preparative regimens prior to stem cells transplantation [39,40]. Attempts to expand the therapeutic applications of rhenium, in order to include solid tumors, had limited success. However, ^{188}Re has been preclinically evaluated as a label for, e.g., somatostatin analogues for treatment of neuroendocrine tumors [41], α-melanocyte stimulating hormone peptide analogs (α-MSH) for treatment of melanoma [42], water soluble oligonucleotides (c-MORF) [43] and peptide-based haptens for treatment of colorectal cancer using a pretargeting approach [44].

Earlier, our group has reported ^{186}Re-maGSG-$Z_{HER2:342}$ as a potential affibody conjugate for therapy of HER2 expressing tumors [45]. This conjugate had a low renal retention, but rather high degree of hepatobiliary excretion. Dosimetry evaluation showed that dose to tumor should exceed dose to normal tissues by several folds. However, a high irradiation of the intestines was a major concern and prompted us to further optimize the targeting properties and biodistribution profile of the anti-HER2 affibody molecule for therapeutic application using rhenium isotopes.

In this study we evaluate seven affibody molecules containing the amino acid sequences GGGC ($Z_{HER2:V2}$), GGSC ($Z_{HER2:V3}$), GGEC ($Z_{HER2:V4}$), GGKC ($Z_{HER2:V5}$), GSGC ($Z_{HER2:V6}$), GEGC ($Z_{HER2:V7}$), and GKGC ($Z_{HER2:V8}$), as peptide-based chelators (Fig. 1) at the C-terminus for labeling with ^{188}Re. Evaluation included binding specificity to HER2 receptors, affinity determination, stability of the conjugates and biodistribution profile of the conjugates in normal and tumor bearing mice. The parental anti-HER2 affibody molecule $Z_{HER2:2395}$ containing a KVDC peptide-based chelator at the C-terminus was used as a reference.

2. Experimental section

2.1. Materials

D-gluconic acid sodium salt, ethylenediaminetetraacetic acid (EDTA) and chloroquine disphosphate were from Sigma–Aldrich, tin(II)-chloride dihydrate ($SnCl_2 \times 2H_2O$) and pyridine were from Fluka Chemika. Phosphate buffered saline, pH 7.4 (PBS) was produced in house.^{188}Re was obtained as perrhenate by elution of a ^{188}W/^{188}Re generator with 4 mL sterile 0.9% sodium chloride (both from Polatom, Otwok-Poland). An automated γ-counter with a ~7.6-cm (3-in) NaI(Tl) detector (1480 WIZARD; Wallac Oy) was used to measure radioactivity. A Cyclone storage phosphor system and OptiQuant image analysis software (both from Perkin–Elmer) were used to measure the radioactivity on instant thin-layer chromatography silica gel-impregnated (ITLC SG) strips. The affibody molecule $Z_{HER2:2395}$ was provided and purified by Affibody AB. The variants $Z_{HER2:V2}$ to $Z_{HER2:V8}$ were produced and purified using a novel antiidiotypic purification strategy, which has been developed earlier by Wållberg et al. [46]. Purity of all variants was above 95%. A description of some relevant properties of these variants is presented elsewhere [35,36]. Data on cellular uptake and biodistribution were assessed by an unpaired, two-tailed Student's *t*-test using GraphPad Prism (v 4.00 for Windows GraphPad Software, San Diego, California, USA) in order to determine any significant differences ($p < 0.05$).

2.2. Labeling of affibody molecules with ^{188}Re

The cysteine-containing HER2-binding affibody molecules were site-specifically labeled with ^{188}Re using freeze-dried labeling kits each containing 5 mg of sodium gluconate, 100 μg of edetate disodium (EDTA), and 1 mg of tin(II) chloride dihydrate. The freeze-dried kits were stored at −20 °C.

Radiolabeling was performed by adding the contents of one freeze-dried kit, dissolved in 1.25 M sodium acetate, pH 4.2, 100 μg of each affibody molecule up to a total volume of 100 μL. To the reaction solution, 35 μL (3–4 MBq) of a ^{188}Re-containing generator eluate was added under argon gas. An equivalent of 220 μg ascorbic acid (2 mg/mL in 1.25 M sodium acetate buffer, pH 4.2) was added to the reaction vial and the mixture was incubated at 90 °C for 60 min and then cooled at room temperature for 5 min. Thereafter, the total amount of ascorbic acid in the reaction vial was adjusted to be 1 mg using a solution of 5 mg/mL ascorbic acid in PBS containing 2% BSA. One μL samples were taken for analysis of the labeling yield by ITLC SG with PBS as the mobile phase. The labeled conjugates were purified using disposable NAP-5 columns (GE Healthcare) pre-equilibrated with PBS, containing 2% BSA. The column was eluted with 900 μL of the same solution. The final solution was further diluted with 100 μL PBS containing 2% BSA and 500 μg ascorbic acid to a final volume of 1 mL. After purification, the purity was evaluated using instant thin-layer chromatography.

2.3. In vitro studies

2.3.1. Binding specificity of radiolabeled affibody molecules to HER2-expressing cells in vitro

Binding specificity of eight ^{188}Re-labeled variants was evaluated using ovarian carcinoma SKOV-3 (1.6×10^6 receptors/cell) purchased from American Type Tissue Culture Collection (ATCC). Cells

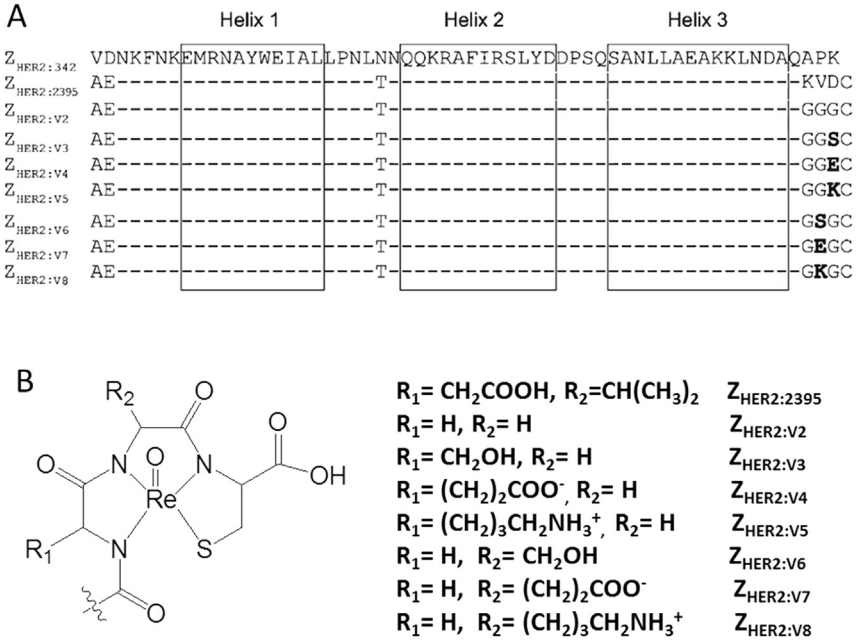

Fig. 1. Overview of the ^{188}Re-labeled affibody molecule variants evaluated in this study. A. The studied HER2-binding affibody molecules including the C-terminal chelating sequence aligned to the parent molecule $Z_{HER2:342}$. The variable amino acids are marked in bold. Positions of α-helices 1 through 3 are indicated by boxes. B. General structure of the N_3S chelators formed by a C-terminal cysteine and three adjacent amino acids. R1 and R2 and denote the side chains of the amino acids involved in the coordination of the radionuclide.

were maintained in Roswell Park Memorial Institute (RPMI) medium (Sigma–Aldrich) containing 10% fetal bovine serum. Briefly, a 2 nM solution of each variant was added to six Petri dishes (~1×10^6 cells/dish). For blocking, a 500-fold excess of non-labeled recombinant $Z_{HER2:2395}$ was added 5 min before the labeled conjugates to saturate the receptors. The cells were incubated during 1 h in a humidified incubator at 37 °C. Thereafter, the media was collected, the cells were detached by trypsin-EDTA solution and the radioactivity in cells and media was measured to calculate the percentage of cell-bound radioactivity.

2.3.2. Affinity determination using LigandTracer

SKOV-3 cells were seeded on a local area of a cell culture dish (NunclonTM, Size 100620, NUNC A/S, Roskilde, Denmark), as described previously [47]. The binding of ^{188}Re-labeled anti-HER2 affibody molecules to living cells was monitored in real-time using LigandTracer Yellow, using established methods [47]. To suppress internalization of affibody-HER2 complex, measurements were performed at 4 °C. By using the TraceDrawer software, which allows the calculation of both association and dissociation rate, it becomes possible to determine the affinity of radiolabeled conjugate [47]. In order to cover the concentration span needed for proper affinity estimation, two concentrations of 49 pM and 98 pM (selected based on previous K_D values obtained using Biacore) of each variant were added in each affinity assay.

2.3.3. Cellular retention of ^{188}Re –labeled affibody molecules by HER2 expressing ovarian carcinoma (SKOV-3) cells

Cellular retention was studied using the methods validated for affibody molecules earlier [20]. SKOV-3 cells (1×10^6 cells/dish) were incubated with 2 nM solution of labeled affibody at 4 °C. After 1 h incubation, the medium with the labeled compound was removed and cells were washed three times with ice-cold serum-free medium. One mL of complete media was added to each dish and cells were further incubated at 37 °C in an atmosphere containing 5% CO_2. At designated time points (4 h and 24 h), a group of three dishes was removed from the incubator, the media was collected and cells were washed three times with ice-cold serum-free medium. Thereafter, cells were detached by trypsin-EDTA solution and the radioactivity in cells and media was measured to calculate the percentage of cell-bound radioactivity from total added.

2.4. In vivo studies

The animal experiments were planned and performed in accordance with national legislation on laboratory animal protection. The animal study plans have been approved by the local Ethics Committee for Animal Research in Uppsala.

Biodistribution studies were performed in female immunocompetent Naval Medical Research Institute (NMRI) mice. All mice were acclimatized for 1 week at the Rudbeck Laboratory animal facility before any experimental procedures. Sixty four mice with an average weight of 30 g were randomized into groups of four animals each. Animals were injected intravenously with 1 μg (120 kBq) conjugate per animal in 100 μL PBS containing 2% BSA. One group of mice was euthanized at each predetermined time point (1 and 4 h after injection) by an intraperitoneal injection of anesthesia, Ketalar–Rompun solution (20 μL/g body weight; Ketalar: 10 mg/mL, Pfizer; Rompun[xylazine]: 1 mg/mL) with subsequent exsanguination by heart puncture using a 1 mL syringe prewashed with diluted heparin (5000 IU/mL). Blood, lung, liver, spleen, stomach, kidney, salivary glands, muscle, bone, intestines, and the remaining carcass were collected. Organs and tissue samples were weighed, and their radioactivity was measured. The tissue uptake values were calculated as percent of injected dose per gram tissue (%ID/g) except for the intestines and the carcass, which were calculated as %ID per whole sample.

In vivo imaging was performed to obtain a visual confirmation of the biodistribution data. Three NMRI mice were injected with 0.7 MBq (8 μg) of ^{188}Re-$Z_{HER2:2395}$ (-KVDC), ^{188}Re-$Z_{HER2:V4}$ (-GGEC) and ^{188}Re-$Z_{HER2:V2}$ (-GGGC) respectively. Mice were sacrificed by cervical dislocation at 4 h after injection. The imaging experiment was performed using an Infinia γ-camera (GE Healthcare) equipped with a High-energy general purpose (HEGP) collimator. Static images (30 min) were obtained with a zoom factor of 2 in a 256 × 256 matrix.

The ^{188}Re-labeled conjugates with the lowest and highest uptake in normal organs, ^{188}Re-$Z_{HER2:V2}$ (-GGGC) and ^{188}Re-$Z_{HER2:2395}$ (-KVDC), respectively, was used in a tumor targeting study with the aim of determining tumor and kidney accumulation of radioactivity. A total of eight Balb/C nude mice (average weight 19 g) were subcutaneously injected with 1×10^7 HER2-expressing SKOV-3 cells in the left flank. Three weeks after implantation the tumors were 3 mm [3] in size and mice were randomized in to two groups ($n = 4$). Each group was injected intravenously with either ^{188}Re-$Z_{HER2:V2}$ (-GGGC) or ^{188}Re-$Z_{HER2:2395}$ (-KVDC) (total protein dose 5 μg per animal, about 90 kBq in 100 μL PBS containing 2% BSA). Mice were sacrificed at 4 h p.i. and previously mentioned organs in addition to the tumors were collected, weighed, and their radioactivity was measured. For specificity control, one additional group ($n = 4$) was pre-injected with 500 μg of $Z_{HER2:342}$ 45 min before injection of ^{188}Re-$Z_{HER2:V2}$ to saturate HER2 receptors in tumors. The animals were sacrificed at 4 h p.i., and uptake in blood and tumors was measured.

3. Results

3.1. Labeling

All affibody molecules were efficiently labeled with ^{188}Re by transchelation from gluconate.

Data concerning the labeling yield and radiochemical purity of $Z_{HER2:2395}$ and the –GXYC variants; $Z_{HER2:V2}$ to $Z_{HER2:V8}$, are presented in Table 1. The labeling yields exceeded 95% for all variants except $Z_{HER2:2395}$ for which the labeling yield was 89.3 ± 1.2%. The radiochemical purity of the labeled products after purification using NAP-5 columns was above 99% for all the eight conjugates.

3.2. Binding to HER2-expressing cells in vitro

All conjugates showed specific binding to the HER2 receptor as the uptake by SKOV-3 cells was significantly (p-value $< 5 \times 10^{-4}$) reduced by pre-saturation with 500-fold molar excess of unlabeled protein.

Table 1
Radiochemical yield and radiochemical purity of different anti-HER2 affibody molecules.

Variant	Yield%	Purity%
^{188}Re-$Z_{HER2:2395}$	89.3 ± 1.2	99.9
^{188}Re-$Z_{HER2:V2}$	95.8 ± 1	100
^{188}Re-$Z_{HER2:V3}$	96.6 ± 0.6	100
^{188}Re-$Z_{HER2:V6}$	97 ± 0.8	100
^{188}Re-$Z_{HER2:V4}$	98.2 ± 0.7	100
^{188}Re-$Z_{HER2:V7}$	95.8 ± 0.1	100
^{188}Re-$Z_{HER2:V5}$	96.5 ± 0.2	100
^{188}Re-$Z_{HER2:V8}$	96.5 ± 0.1	100

The kinetics measurements of all the eight ^{188}Re-labeled affibody molecules binding to HER2-expressing SKOV-3 cells in vitro using LigandTracer confirmed that high affinity to HER2 was preserved after labeling. Evaluation of data by fitting the binding and dissociation curves to a 1:1 interaction model indicates that the binding of radiolabeled conjugates to living HER2-expressing cells is mediated by single binding site populations. This 1:1 interaction is in agreement with previously obtained Surface Plasmon Resonance (SPR) analysis data performed on a Biacore 2000 instrument (GE Healthcare) [36]. The dissociation constants at equilibrium (K_D) for binding of radiolabeled affibody molecules to the HER2 receptor are shown in Table 2. All variants demonstrated high affinity in the low picomolar range. Fig. 2 shows the K_D measurement sensogram for ^{188}Re-$Z_{HER2:V2}$.

The composition of the peptide-based chelators had an apparent influence on the cellular retention of the ^{188}Re-labeled conjugates after binding to HER2-expressing SKOV-3 cells (Fig. 3).^{188}Re-$Z_{HER2:2395}$ and ^{188}Re-$Z_{HER2:V5}$ (both containing the positively charged amino acid lysine) showed the highest overall retention compared to the other variants, ^{188}Re-$Z_{HER2:V3}$ (-GGSC) and ^{188}Re-$Z_{HER2:V4}$ (-GGEC) containing a polar and a negatively charged amino acid, respectively, showed moderate overall retention after 24 h. ^{188}Re-$Z_{HER2:V2}$ (-GGGC) with no polar or charged residues had the lowest overall retention both at 4 and 24 h. Moreover, $Z_{HER2:V6}$ (-GSGC), $Z_{HER2:V7}$ (-GEGC) and $Z_{HER2:V8}$ (-GKGC) showed an appreciable difference from the levels of cellular retention obtained for their counterparts with GGXC chelators ($Z_{HER2:V3}$, $Z_{HER2:V4}$ and $Z_{HER2:V5}$). In general, the GXGC-containing conjugates were less efficiently retained by HER2 expressing cells.

3.3. In vivo studies

To determine the *in vivo* uptake of radioactivity in different organs, the radiolabeled constructs were injected into female NMRI mice. Data concerning biodistribution 1 and 4 h p.i, are presented in Table 3. For comparison, data of the GXGC and GGXC-containing counterparts are provided in the form of pairs. All comparative findings reported are statistically significant unless otherwise stated. All eight studied ^{188}Re-labeled constructs, $Z_{HER2:2395}$, $Z_{HER2:V2}$, $Z_{HER2:V3}$, $Z_{HER2:V6}$, $Z_{HER2:V4}$, $Z_{HER2:V7}$, $Z_{HER2:V5}$ and $Z_{HER2:V8}$ showed a rapid blood clearance, which is typical for affibody molecules. The blood-associated radioactivity was reduced 5–8.2-fold between 1 and 4 h after injection. A low level of radioactivity in the gastrointestinal tract (with its content) suggested that hepatobiliary excretion did not play a substantial role. No significant differences in radioactivity were observed in organs that rapidly establish an equilibrium with the blood pool (spleen and salivary glands). All other non-excretory organs displayed similar uptake profiles of the different affibody variants.

Overall, the analysis demonstrated a strong influence of the composition of the peptide-based chelator and the relative positions of amino acids on the biodistribution. Most obvious was the influence on uptake in liver, lung and kidneys (Fig. 4). It is apparent that the lysine containing variants ^{188}Re-$Z_{HER2:2395}$ (KVDC), ^{188}Re-$Z_{HER2:V5}$ (GGKC) and ^{188}Re-$Z_{HER2:V8}$ (GKGC) were retained to a higher extent in the excretory organs in comparison to other variants. Moreover, changing the position of a single amino acid on the peptide based chelator from GGXC to GXGC resulted in a significantly lower retention in the liver (1.44 ± 0.06 %ID/g for $Z_{HER2:V3}$ vs. 0.7 ± 0.1%ID/g for $Z_{HER2:V6}$, 1.3 ± 0.3 %ID/g for $Z_{HER2:V4}$ vs. 0.8 ± 0.1 %ID/g for $Z_{HER2:V7}$ and 3.3 ± 0.5%ID/g for $Z_{HER2:V5}$ vs. 2.4 ± 0.1 %ID/g for $Z_{HER2:V8}$) and kidneys (20 ± 4 %ID/g for $Z_{HER2:V3}$ vs. 10 ± 1 %ID/g for $Z_{HER2:V6}$, 31 ± 6 %ID/g for $Z_{HER2:V4}$ vs. 23 ± 2 %ID/g for $Z_{HER2:V7}$ and 152 ± 24 %ID/g for $Z_{HER2:V5}$ vs. 136 ± 23 %ID/g for $Z_{HER2:V8}$) at 4 h after injection. A somewhat elevated lung uptake of ^{188}Re-$Z_{HER2:V4}$ was observed both at 1 and 4 h after injection (3.2 ± 0.8 and 1.0 ± 0.3 %ID/g respectively), compared to the other variants. This elevated pulmonary uptake has been observed earlier for ^{99m}Tc-labeled $Z_{HER2:V4}$ at 4 h p.i. [35]. Throughout the study the variant, ^{188}Re-$Z_{HER2:V2}$, with the C-terminal chelating sequence –GGGC, provided the lowest radioactivity retention in all organs including the kidneys (3.1 ± 0.5 %ID/g 4 h p.i.) and liver (0.33 ± 0.05 %ID/g 4 h p.i.).

A comparative imaging study using ^{188}Re-$Z_{HER2:2395}$, ^{188}Re-$Z_{HER2:V4}$ and ^{188}Re-$Z_{HER2:V2}$ respectively confirmed the biodistribution results (Fig. 5). Images obtained at 4 h after injection showed no visible uptake in any organ except from kidneys. The intensity of kidney visualization varied between ^{188}Re-$Z_{HER2:2395}$ (strong) and ^{188}Re-$Z_{HER2:V4}$ (moderate). The kidneys were barely visible when mice were injected with ^{188}Re-$Z_{HER2:V2}$.

To evaluate influence of chelators on tumor targeting, we performed a comparative biodistribution study between ^{188}Re-$Z_{HER2:V2}$ and ^{188}Re-$Z_{HER2:2395}$ in female NMRI nu/nu mice bearing subcutaneous SKOV-3 ovarian carcinoma xenografts. The mice were sacrificed at 4 h after injection. Data are presented in Table 4. The data of normal organs uptake is in excellent agreement with those obtained in normal NMRI mice (Tables 3 and 4). Moreover, efficient tumor targeting has been demonstrated. The tumor uptake of ^{188}Re-$Z_{HER2:V2}$ (18.7 ± 2.8 %ID/g) exceeded by far the uptake in any other organ or tissue. Tumor uptake exceeded kidney uptake by 5-fold at this time point. As expected, the radioactivity concentration of ^{188}Re-$Z_{HER2:2395}$ exceeded that of ^{188}Re-$Z_{HER2:V2}$ in many organs, especially the kidneys (196 ± 38 vs. 3.4 ± 0.3 %ID/g, respectively) and liver (2.5 ± 0.54 vs. 0.40 ± 0.01 %ID/g, respectively). The overall tumor-to-organ ratios are presented in Table 4 for comparison. To evaluate *in vivo* specificity of HER2 targeting using ^{188}Re-$Z_{HER2:V2}$, HER2 receptors in tumors were saturated in a group of mice by pre-injection of large excess of non-labeled parental $Z_{HER2:342}$ affibody molecule. Tumor uptake in this group was 2.2 ± 1.8 %ID/g, which is significantly ($p < 0.05$) lower than uptake in the non-blocked group (18.7 ± 2.8 %ID/g). The blood concentration (0.18 ± 0.04 %ID/g) did not differ significantly from the concentration in the non-blocked group. The results of this experiment demonstrate saturability of HER2 targeting *in vivo* and suggest its specificity.

Table 2
The dissociation constants K_D of interaction of rhenium-188 labeled affibody molecules with HER2-expressing SKOV-3 cells determined using LigandTracer at 4 °C.

Affinity determination using ligand tracer	
Variant	K_D (pM)
^{188}Re-$Z_{HER2:2395}$	10.6 ± 0.6
^{188}Re-$Z_{HER2:V2}$	6.4 ± 0.4
^{188}Re-$Z_{HER2:V3}$	51 ± 3
^{188}Re-$Z_{HER2:V6}$	4 ± 1
^{188}Re-$Z_{HER2:V4}$	10 ± 6
^{188}Re-$Z_{HER2:V7}$	21 ± 10
^{188}Re-$Z_{HER2:V5}$	5 ± 2
^{188}Re-$Z_{HER2:V8}$	<13 pM[a]

[a] Accurate measurement of off-rate was not possible despite 6 h long measurement due to very slow dissociation.

4. Discussion

High renal reabsorption of affibody molecules is the major issue in development of conjugates for radionuclide therapy. The use of residualizing labels results in that the a renal uptake is exceeding the tumor uptake by 15–20 fold, which makes radionuclide therapy non-feasible [16,34,48]. One approach for the development of

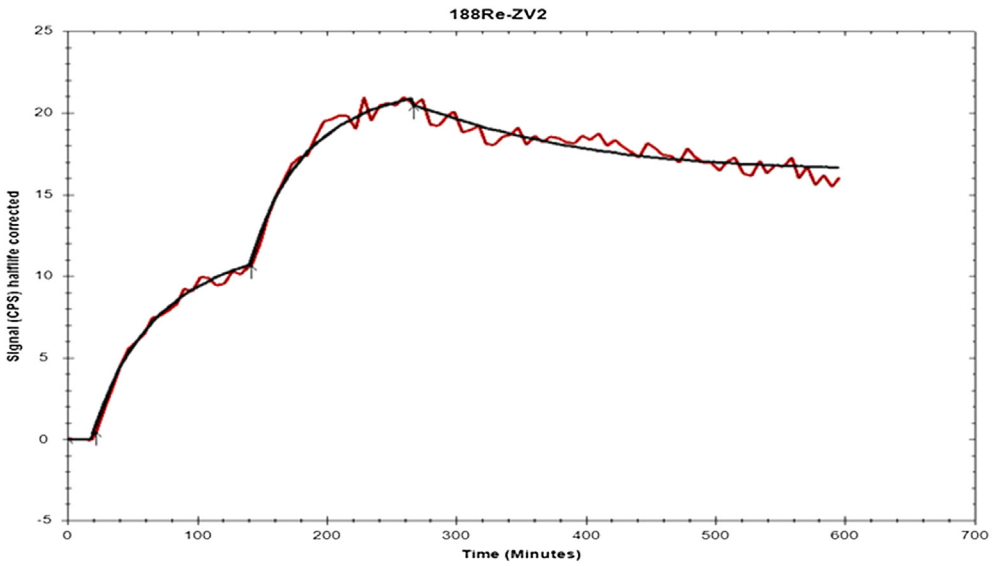

Fig. 2. Sensorgram of ^{188}Re-$Z_{HER2:V2}$ dissociation constants at equilibrium (K_D) for binding of radiolabeled affibody molecules to HER2 expressing SKOV-3 cells using LigandTracer Yellow with two different concentrations at 4 °C.

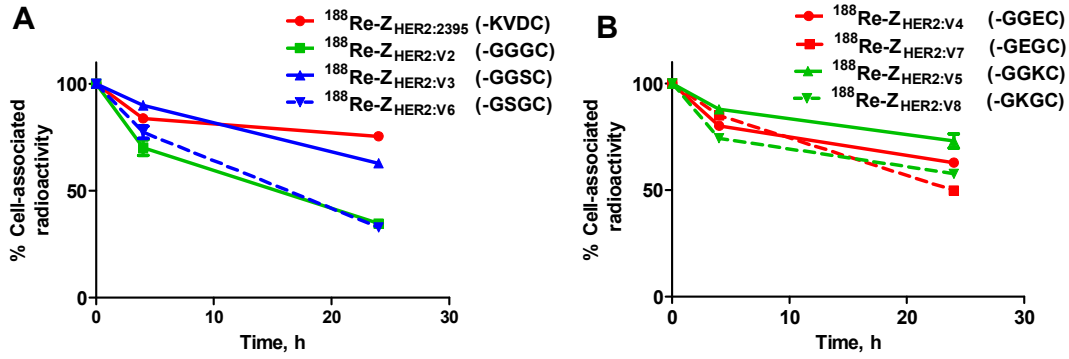

Fig. 3. Influence of the amino acid composition and their position in the cysteine-containing chelators on the cellular retention of ^{188}Re-labeled affibody molecules by SKOV-3 cells. A. retention of ^{188}Re-$Z_{HER2:2395}$ (-KVDC), ^{188}Re-$Z_{HER2:V2}$ (-GGGC), ^{188}Re-$Z_{HER2:V3}$ (-GGSC), ^{188}Re-$Z_{HER2:V3}$ (-GSGC); B. retention of ^{188}Re-$Z_{HER2:V4}$ (-GGEC), ^{188}Re-$Z_{HER2:V7}$ (-GEGC), ^{188}Re-$Z_{HER2:V5}$ (-GGKC), ^{188}Re-$Z_{HER2:V8}$ (-GKGC).

therapeutic conjugates is based on different cellular processing of affibody molecules by tumor cells (slow internalization) and by cell in proximal tubuli in kidneys (rapid internalization). The use of non-residualizing labels provides a rapid clearance of radioactivity from kidneys but slow release from tumors due to a high affinity to the target. This permits obtaining higher radioactivity concentration in tumors than in kidneys and should thus make radionuclide therapy using affibody molecules possible [26,45]. Previous studies have demonstrated that the composition of cysteine-containing peptide-based chelators might be used for modulation of renal uptake of ^{99m}Tc and provided higher uptake in tumors than in kidneys [35,36]. The chemical similarity between Re and Tc creates a potential for translation of this approach to the development of therapeutic targeting agents. However, the properties of rhenium and technetium are not identical, and substituting ^{99m}Tc with rhenium radioisotopes might appreciably influence the blood clearance rate, as well as the uptake and retention in excretory organs and other tissues [41,45]. This necessitates a re-evaluation of the influence of peptide-based chelators on the uptake and retention of ^{188}Re-labeled affibody molecules in liver and kidneys.

Peptide-based cysteine-containing chelators are directly engineered into the affibody molecules by genetic insertion of peptide-encoding gene fragments, and the constructs can be produced in high yield in prokaryotic hosts, i.e. *E. coli*. No further conjugation step is thus required, which simplifies the process and reduces costs. The labeling is site-specific, which is important to provide a uniform radiolabeled product with reproducible physicochemical and biological properties. This is essential, as our previous studies have demonstrated that the position of the chelators noticeably influences the biodistribution and targeting properties of ^{99m}Tc-labeled affibody molecules [32].

Generally, labeling with rhenium requires much higher concentration of reducing agents than labeling with technetium, and thus harsher labeling conditions [41]. These conditions are generally non-compatible with proteins that are dependent on disulfide bonds, such as antibodies and antibody fragments. To overcome this, an indirect two-step process was developed for labeling of antibodies where rhenium is first chelated by N_3S chelator in harsh conditions, and then the chelator is conjugated to an antibody [49–52]. Multiple steps increase probability of labeling failure and reduces yield. The use of peptide-based chelators permits high-yield labeling (Table 1) of affibody molecules with ^{188}Re in the presence of gluconate as an exchange ligand. Currently, the labeling is performed using a two-vial kit, but it is amenable to development

Table 3
Biodistribution of ^{188}Re –labeled affibody molecules in female NMRI mice, 1 and 4 h after intravenous injection. The measured radioactivity of different organs is expressed as % ID/g, and presented as an average value from 4 animals ± SD.

	^{188}Re-$Z_{HER2:2395}$ (-KVDC)	^{188}Re-$Z_{HER2:V2}$ (-GGGC)	^{188}Re-$Z_{HER2:V3}$ (-GGSC)	^{188}Re-$Z_{HER2:V6}$ (-GSGC)	^{188}Re-$Z_{HER2:V4}$ (-GGEC)	^{188}Re-$Z_{HER2:V7}$ (-GEGC)	^{188}Re-$Z_{HER2:V5}$ (-GGKC)	^{188}Re-$Z_{HER2:V}$ (-GKGC)
1 h								
Blood	1.0 ± 0.1	1.18 ± 0.08	1.31 ± 0.06	1.6 ± 0.1	1.1 ± 0.3	1.5 ± 0.1	1.2 ± 0.1	1.15 ± 0.12
Lung	1.5 ± 0.1	1.9 ± 0.2	2.1 ± 0.2	2.5 ± 0.2	3.2 ± 0.8	2.0 ± 0.2	2.47 ± 0.45	2.0 ± 0.2
Liver	2.57 ± 0.25	1.3 ± 0.1	2.0 ± 0.2	2.0 ± 0.1	1.8 ± 0.3	1.9 ± 0.2	3.2 ± 0.8	2.6 ± 0.2
Spleen	0.7 ± 0.2	0.53 ± 0.04	1.0 ± 0.2	1.1 ± 0.2	1.0 ± 0.3	0.8 ± 0.1	1.25 ± 0.18	1.07 ± 0.07
Stomach	0.9 ± 0.1	1.3 ± 0.3	1.38 ± 0.15	2.0 ± 0.2	1.3 ± 0.4	1.5 ± 0.1	2.2 ± 0.6	1.42 ± 0.15
Kidney	148 ± 13	26 ± 6	94 ± 8	68 ± 7	129 ± 21	121 ± 18	150 ± 19	146 ± 8
Salivary gland	0.6 ± 0.1	0.7 ± 0.05	0.8 ± 0.2	1.0 ± 0.1	0.9 ± 0.3	0.9 ± 0.1	1.3 ± 0.3	0.85 ± 0.1
Muscle	0.30 ± 0.03	0.33 ± 0.02	0.40 ± 0.02	0.38 ± 0.02	0.35 ± 0.05	0.4 ± 0.1	0.4 ± 0.05	0.4 ± 0.1
Bone	1.1 ± 0.1	0.9 ± 0.3	1.0 ± 0.1	1.1 ± 0.1	1.0 ± 0.2	1.1 ± 0.2	1.16 ± 0.25	0.9 ± 0.2
Carcass[a]	9.7 ± 1.3	10 ± 0.3	11 ± 1.0	14 ± 1.3	10.6 ± 1.6	12 ± 1.0	11.3 ± 0.8	10.2 ± 0.5
GI tract[a]	3.4 ± 0.3	1.5 ± 0.2	1.9 ± 0.3	2.18 ± 0.35	1.6 ± 0.2	1.8 ± 0.1	2.1 ± 0.2	1.9 ± 0.2
4 h								
Blood	0.14 ± 0.04	0.15 ± 0.03	0.28 ± 0.05	0.20 ± 0.02	0.2 ± 0.1	0.18 ± 0.05	0.19 ± 0.05	0.20 ± 0.06
Lung	0.5 ± 0.1	0.24 ± 0.09	0.66 ± 0.07	0.40 ± 0.03	1.0 ± 0.3	0.4 ± 0.1	1.0 ± 0.2	0.8 ± 0.1
Liver	2.23 ± 0.46	0.33 ± 0.05	1.44 ± 0.06	0.7 ± 0.1	1.3 ± 0.3	0.8 ± 0.1	3.3 ± 0.5	2.45 ± 0.12
Spleen	0.5 ± 0.1	0.16 ± 0.03	0.5 ± 0.1	0.33 ± 0.08	0.47 ± 0.15	0.3 ± 0.1	0.8 ± 0.4	0.8 ± 0.1
Stomach	0.55 ± 0.15	0.5 ± 0.3	1.0 ± 0.4	0.7 ± 0.2	0.6 ± 0.4	0.33 ± 0.03	1.5 ± 0.5	0.75 ± 0.20
Kidney	172 ± 32	3.1 ± 0.5	20 ± 4.0	10 ± 1.0	31 ± 6	23 ± 2	152 ± 24	136 ± 23
Salivary gland	0.4 ± 0.1	0.29 ± 0.16	0.56 ± 0.05	0.55 ± 0.06	0.42 ± 0.20	0.25 ± 0.02	0.80 ± 0.35	0.65 ± 0.12
Muscle	0.11 ± 0.01	0.05 ± 0.01	0.13 ± 0.04	0.07 ± 0.02	0.09 ± 0.03	0.06 ± 0.01	0.15 ± 0.03	0.12 ± 0.01
Bone	0.8 ± 0.3	0.22 ± 0.05	0.3 ± 0.1	0.21 ± 0.05	0.34 ± 0.07	0.26 ± 0.03	0.6 ± 0.2	0.47 ± 0.04
Carcass[a]	3.4 ± 0.5	1.8 ± 0.4	4.1 ± 0.5	2.7 ± 1.2	2.82 ± 0.55	2.3 ± 0.2	5.3 ± 0.9	4.2 ± 0.8
GI tract[a]	3.1 ± 0.2	1.89 ± 1.45	1.7 ± 0.6	2.6 ± 0.8	2.5 ± 1.5	1.6 ± 0.5	1.8 ± 0.3	1.4 ± 0.8

[a] Data for gastro-intestinal tract with content and carcass are presented as % of injected radioactivity per whole sample.

of single-vial kit, which would further increase robustness of the procedure [53]. In addition to the small size and rapid kinetics of affibody molecules, their tolerance to harsh labeling conditions (robustness) is a major advantage over immunoglobulin-based targeting agents. All the eight ^{188}Re-labeled affibody molecules bound to HER2-expressing cells with high (low picomolar) affinity (Table 2).

The amino acids adjacent to cysteine had a clear effect on the cellular processing of ^{188}Re-labeled affibody molecules. The cellular retention was the highest for lysine-containing chelators, followed by glutamate- and serine-containing ones (Fig. 3). For each pair of homologous chelators, the GGXC variants (where X = K, E or S) provided better retention of radioactivity than the GXGC counterparts (Fig. 3). This pattern was in excellent agreement with our earlier data concerning cellular processing of ^{99m}Tc-labeled variants [36]. As affinities of binding to HER2-expressing cells were very similar for all variants (Table 2), the difference in cellular retention was, most likely, due to difference in cellular processing of radiocatabolites after internalization and lysosomal degradation. This is supported by close resemblance of retention profiles of ^{188}Re-$Z_{HER2:V2}$ and ^{188}Re-$Z_{HER2:V3}$ with the profile of the parental affibody labeled with non-residualizing radioiodine labels [54], while retention pattern of ^{188}Re-$Z_{HER2:2395}$, ^{188}Re-$Z_{HER2:V5}$ and ^{188}Re-$Z_{HER2:V8}$ was similar to the profile of affibody molecules labeled with residualizing ^{111}In [48]. Despite the lower retention by SKOV-3 cells, the biological half-life of ^{188}Re-$Z_{HER2:V2}$ and ^{188}Re-$Z_{HER2:V3}$ was about 15 h, which corresponds well with retention of radioactivity delivered by affibody molecules with non-residualizing radiohalogen labels to HER2-expressing tumors *in vivo* [26,54].

In vivo data suggest rapid clearance of all conjugates from blood (Table 3). The radioactivity uptake in the gastrointestinal tract (with content) was low, typically less than 2% of injected radioactivity. This suggests that the hepatobiliary pathway played a minor role, if any, in the excretion of the conjugates or their radiometabolites. The radioactivity uptake in Na/I symporter expressing organs, stomach and salivary gland, was also low. Since these organs accumulate radioperrhenate [55], the low uptake indicates that there was no loss of the radionuclide *in vivo* due to re-oxidation of ^{188}Re. Uptake in muscle and bone was also low, and variation between conjugates was not substantial. However, the retention of constructs with lysine-containing chelators (i.e. ^{188}Re-$Z_{HER2:2395}$, ^{188}Re-$Z_{HER2:V5}$ and ^{188}Re-$Z_{HER2:V8}$) was significantly higher than others. The most apparent was the difference in uptakes in lungs, liver, and kidneys (Fig. 4). Uptake of radioactivity at 4 h p.i. was significantly higher for constructs with GGXC variants (where X = E or S) than for GXGC in lung and kidneys. For liver, this was true also for lysine-containing chelators.

The uptake of ^{188}Re-$Z_{HER2:V2}$ (with GGGC chelator) was lower in all these organs than the uptake of constructs with chelators containing polar or charged side chains. The most striking was the difference in the renal uptake. The renal uptake of ^{188}Re-$Z_{HER2:V2}$ was 2.5–6 fold lower than uptake of other conjugates already at 1 h p.i. At 4 h p.i., the renal uptake of ^{188}Re-$Z_{HER2:V2}$ was 40–50 fold lower than the uptake of constructs with lysine-containing chelators (^{188}Re-$Z_{HER2:2395}$, ^{188}Re-$Z_{HER2:V5}$ and ^{188}Re-$Z_{HER2:V8}$). Overall, the pattern of the radioactivity retention in kidneys resembled the pattern of cellular retention of the same constructs by SKOV-3 cells, i.e. the ranking of conjugates according to their retention was the same, but the magnitude of the variance was different. Most likely, this difference can be explained by that the internalization rate of affibody molecules in kidneys is much higher than in tumor cells. After re-absorption from primary urine in proximal tubuli, affibody molecules should be degraded in lysosomes. The further fate of radiorhenium depends of physiochemical properties of the radiocatabolites. Most likely, radiocatabolites of ^{188}Re-$Z_{HER2:V2}$ leak directly into urine, as biodistribution of this agent does not show any site of their possible re-uptake. This creates preconditions for successful targeted radionuclide therapy of HER2-expressing tumors using ^{188}Re-$Z_{HER2:V2}$.

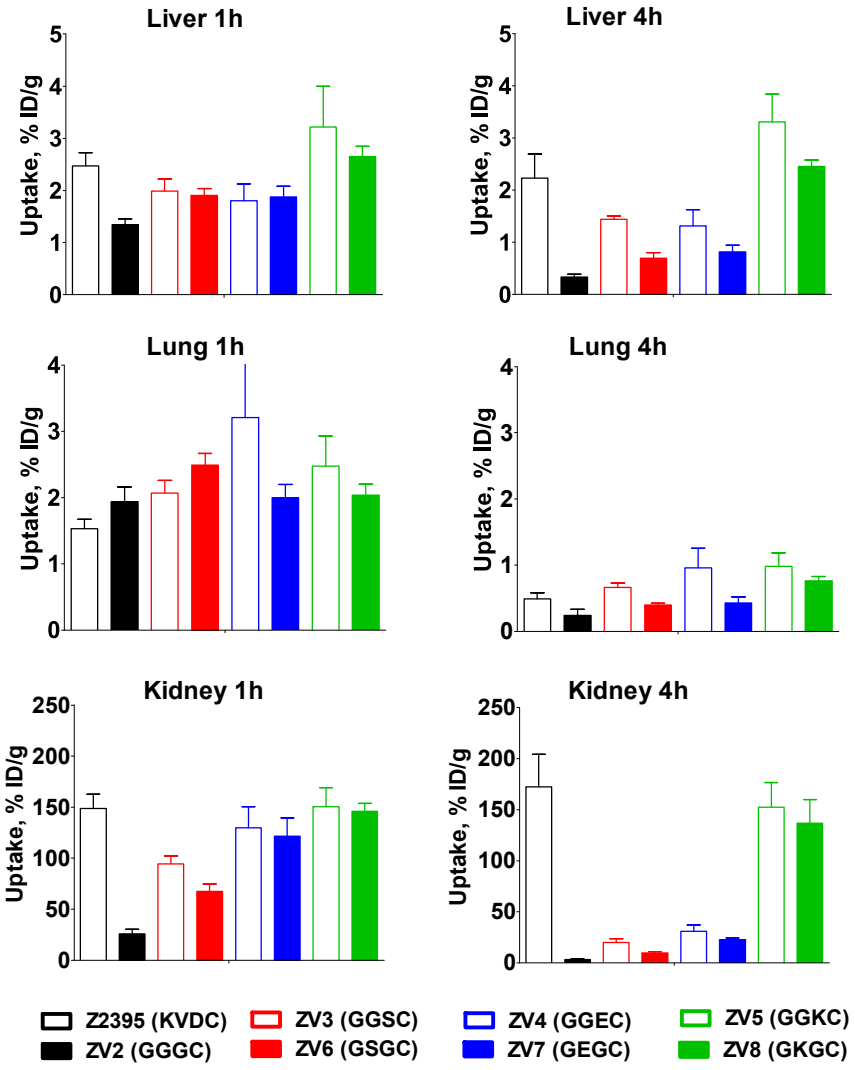

Fig. 4. Influence of composition of the −GXYC peptide-based chelator on the uptake of ^{188}Re -labeled affibody molecules in liver, lung, and kidneys 1 and 4 h after injection. The radioactivity of different organs is expressed as % ID/g and presented as an average value from four animals ± standard deviation.

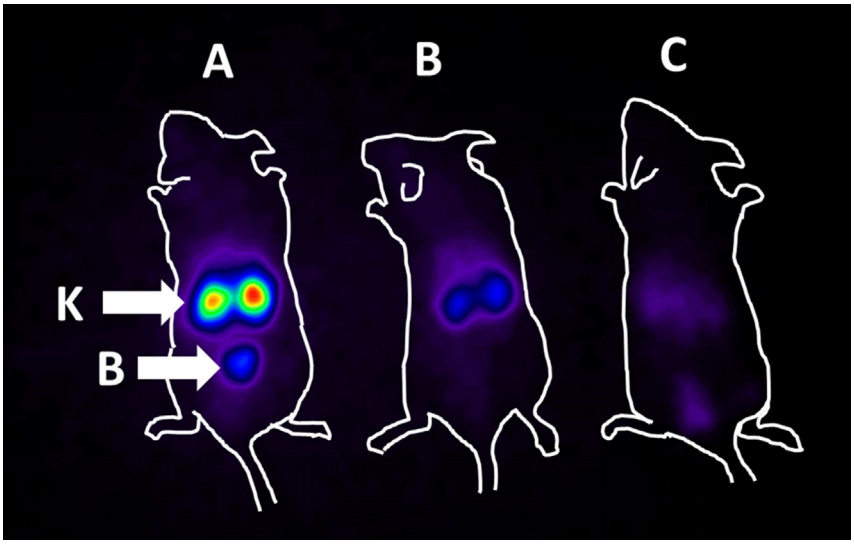

Fig. 5. γ-camera imaging of mice injected with ^{188}Re -labeled $Z_{HER2:2395}$, $Z_{HER2:V2}$ and $Z_{HER2:V4}$ at 4 h p.i. Visualization of kidneys was only possible with $Z_{HER2:2395}$ (A) and $Z_{HER2:V4}$ (B) while it was impossible with $Z_{HER2:V2}$ (C). (K) kidneys, (B) bladder.

Table 4
Comparative biodistribution of ^{188}Re-$Z_{HER2:V2}$ and ^{188}Re-$Z_{HER2:2395}$ in female NMRI nu/nu mice bearing subcutaneous SKOV-3 xenografts at 4 h after intravenous injection. The uptake values are presented as an average value from 4 animals ± SD.

	^{188}Re-$Z_{HER2:V2}$		^{188}Re-$Z_{HER2:2395}$	
	Uptake, % ID/g	Tumor-to-organ ratio	Uptake, % ID/g	Tumor-to-organ ratio
Tumor	18.7 ± 2.8[b]		11.4 ± 4.5	
Blood	0.20 ± 0.15	92	0.22 ± 0.1	53
Lung	0.39 ± 0.01	48	0.8 ± 0.38	14
Liver	0.40 ± 0.01[b]	46	2.5 ± 0.54	5
Spleen	0.22 ± 0.05[b]	84	0.97 ± 0.18	12
Stomach	0.37 ± 0.1	51	0.7 ± 0.25	16
Kidney	3.4 ± 0.30[b]	5	196 ± 38	0.06
Salivary gland	0.26 ± 0.03[b]	70	0.61 ± 0.15	19
Muscle	0.09 ± 0.03	210	0.12 ± 0.01	92
Bone	0.21 ± 0.04[b]	87	0.58 ± 0.10	20
Carcass[a]	2.9 ± 0.62		4.1 ± 0.9	
GI tract[a,b]	0.8 ± 0.12		2.2 ± 0.3	

[a] Data for gastro-intestinal tract with content and carcass are presented as % of injected radioactivity per whole sample.
[b] Significant difference ($p < 0.05$) between ^{188}Re-$Z_{HER2:V2}$ and ^{188}Re-$Z_{HER2:2395}$.

The biodistribution of ^{188}Re-labeled affibody molecules was very similar to the biodistribution of their ^{99m}Tc-labeled counterparts studied earlier [35,36]. However, there were some noticeable differences. For example, the uptake of ^{188}Re-$Z_{HER2:V2}$ was lower in liver and spleen at 4 h p.i. than the uptake of ^{99m}Tc-$Z_{HER2:V2}$. On the other hand, the uptake of ^{188}Re-$Z_{HER2:V3}$ was higher in lung, liver, spleen, stomach and salivary gland than the uptake of ^{99m}Tc-$Z_{HER2:V3}$. Despite their chemical similarity, rhenium and technetium labels have different influence on biodistribution of labeled affibody molecules, necessitating careful structure-properties relationship studies for each label.

The biodistribution of ^{188}Re-$Z_{HER2:V2}$ in mice bearing HER2-expressing tumor xenografts (Table 4) demonstrated that tumor uptake at 4 h after injection appreciably exceeded uptake in any other organs. In vivo blocking experiment demonstrated HER2 specificity of targeting SKOV-3 xenografts using ^{188}Re-$Z_{HER2:V2}$. Uptake in blood and bone, which are associated with bone marrow suppression, were 90-fold lower than the tumor uptake. Renal uptake was 5-fold lower that the uptake in tumors. This suggests that ^{188}Re-$Z_{HER2:V2}$ can efficiently target HER2-expressing tumors and justifies its further development as a targeting agent for radionuclide therapy.

Earlier, we have studied synthetically produced anti-HER2 affibody molecules, maGGG-$Z_{HER2:342}$ and maGSG-$Z_{HER2:342}$ labeled with ^{186}Re on the N-terminus [45]. Both ^{186}Re- maGGG and ^{186}Re-maGSG with non-residualizing labels provided low retention of radioactivity in kidneys, making radionuclide therapy possible. However, the placement of the label at the C-terminus in the current study resulted in a 10-fold reduction of hepatobiliary excretion of radioactivity, which reduces the dose to the radiosensitive intestines. Thus, ^{188}Re-$Z_{HER2:V2}$ is a better format for affibody molecules aimed for therapy.

In conclusion, ^{188}Re-$Z_{HER2:V2}$ provides lower retention of radioactivity in kidneys, and is a promising candidate for radionuclide therapy of HER2-expressing tumors. This study, along with other studies on affibody molecules, suggests that an optimal labeling strategy permits not only a stable attachment of a radionuclide to a targeting scaffold protein, but also allows for optimization of biodistribution and targeting properties of the radioconjugate.

Acknowledgment

This research was financially supported by grants from Swedish Cancer Society (Cancerfonden) 2011/483 and 2012/352 and Swedish Research Council (Vetenskapsrådet) 2012-163 and 2012-2228.

References

[1] T.A. Bailey, H. Luan, R.J. Clubb, M. Naramura, V. Band, S.M. Raja, H. Band, Mechanisms of Trastuzumab resistance in ErbB2-driven breast cancer and newer opportunities to overcome therapy resistance, J. Carcinog. 10 (2011) 28.
[2] T.M. Brand, M. Iida, D.L. Wheeler, Molecular mechanisms of resistance to the EGFR monoclonal antibody cetuximab, Cancer Biol. Ther. 11 (2011) 777–792.
[3] G. Giaccone, Y. Wang, Strategies for overcoming resistance to EGFR family tyrosine kinase inhibitors, Cancer Treat. Rev. 37 (2011) 456–464.
[4] Y.C. Wang, G. Morrison, R. Gillihan, J. Guo, R.M. Ward, X. Fu, M.F. Botero, N.A. Healy, S.G. Hilsenbeck, G.L. Phillips, G.C. Chamness, M.F. Rimawi, C.K. Osborne, R. Schiff, Different mechanisms for resistance to trastuzumab versus lapatinib in HER2-positive breast cancers–role of estrogen receptor and HER2 reactivation, Breast Cancer Res. 13 (2011) R121.
[5] H. Daub, K. Specht, A. Ullrich, Strategies to overcome resistance to targeted protein kinase inhibitors, Nat. Rev. Drug Discov. 3 (2004) 1001–1010.
[6] W.F. Bale, I.L. Spar, R.L. Goodland, Experimental radiation therapy of tumors with I131-carrying antibodies to fibrin, Cancer Res. 20 (1960) 1488–1494.
[7] R. Hiramoto, Y. Yagi, D. Pressman, In vivo fixation of antibodies in the adrenal, Proc. Soc. Exp. Biol. Med. 98 (1958) 870–874.
[8] R.M. Sharkey, D.M. Goldenberg, Perspectives on cancer therapy with radiolabeled monoclonal antibodies, J. Nucl. Med. 46 (2005) 115S–127S.
[9] V. Kenanova, A.M. Wu, Tailoring antibodies for radionuclide delivery, Expert Opin. Drug Deliv. 3 (2006) 53–70.
[10] J.J. Teunissen, D.J. Kwekkeboom, M. de Jong, J.P. Esser, R. Valkema, E.P. Krenning, Endocrine tumours of the gastrointestinal tract. Peptide receptor radionuclide therapy, Best Pract. Res. Clin. Gastroenterol. 19 (2005) 595–616.
[11] D.M. Goldenberg, J.F. Chatal, J. Barbet, O. Boerman, R.M. Sharkey, Cancer imaging and therapy with bispecific antibody pretargeting, Update Cancer Ther. 2 (2007) 19–31.
[12] P.A. Nygren, Alternative binding proteins: affibody binding proteins developed from a small three-helix bundle scaffold, FEBS J. 275 (2008) 2668–2676.
[13] J. Löfblom, J. Feldwisch, V. Tolmachev, J. Carlsson, S. Ståhl, F.Y. Frejd, Affibody molecules: engineered proteins for therapeutic, diagnostic and biotechnological applications, FEBS Lett. 584 (2010) 2670–2680.
[14] A. Orlova, J. Feldwisch, L. Abrahmsén, V. Tolmachev, Update: affibody molecules for molecular imaging and therapy for cancer, Cancer Biother. Radiopharm. 22 (2007) 573–584.
[15] P. Arora, T.G. Oas, J.K. Myers, Fast and faster: a designed variant of the B domain of protein A folds in 3 microsec, Protein Sci. 13 (2004) 847–853.
[16] M. Altai, J. Strand, D. Rosik, R.K. Selvaraju, A. Eriksson Karlström, A. Orlova, V. Tolmachev, Influence of nuclides and chelators on imaging using affibody molecules: comparative evaluation of recombinant affibody molecules site-specifically labeled with ^{68}Ga and ^{111}In via maleimido derivatives of DOTA and NODAGA, Bioconjug. Chem. 24 (2013) 1102–1109.
[17] T. Tran, T. Engfeldt, A. Orlova, M. Sandström, J. Feldwisch, L. Abrahmsén, A. Wennborg, V. Tolmachev, A.E. Karlström, (99m)Tc-maEEE-Z(HER2:342), an Affibody molecule-based tracer for the detection of HER2 expression in malignant tumors, Bioconjug. Chem. 18 (2007) 1956–1964.
[18] S. Heskamp, P. Laverman, D. Rosik, F. Boschetti, W.T. van der Graaf, W.J. Oyen, H.W. van Laarhoven, V. Tolmachev, O.C. Boerman, Imaging of human epidermal growth factor receptor type 2 expression with 18F-labeled affibody molecule ZHER2:2395 in a mouse model for ovarian cancer, J. Nucl. Med. 53 (2012) 146–153.
[19] A. Orlova, M. Magnusson, T.L. Eriksson, M. Nilsson, B. Larsson, I. Höidén-Guthenberg, C. Widström, J. Carlsson, V. Tolmachev, S. Ståhl, F.Y. Nilsson, Tumor imaging using a picomolar affinity HER2 binding affibody molecule, Cancer Res. 66 (2006) 4339–4348.
[20] H. Wållberg, A. Orlova, Slow internalization of anti-HER2 synthetic affibody monomer 111In-DOTA-ZHER2:342-pep2: implications for development of labeled tracers, Cancer Biother. Radiopharm. 23 (2008) 435–442.
[21] V. Tolmachev, A. Orlova, R. Pehrson, J. Galli, B. Baastrup, K. Andersson, M. Sandström, D. Rosik, J. Carlsson, H. Lundqvist, A. Wennborg, F.Y. Nilsson, Radionuclide therapy of HER2-positive microxenografts using a 177Lu-labeled HER2-specific Affibody molecule, Cancer Res. 67 (2007) 2773–2782.
[22] M.A. Fortin, A. Orlova, P.U. Malmström, V. Tolmachev, Labelling chemistry and characterization of [90Y/177Lu]-DOTAZHER2:342–3 Affibody molecule, a candidate agent for locoregional treatment of urinary bladder carcinoma, Int. J. Mol. Med. 19 (2007) 285–291.
[23] A. Orlova, D. Rosik, M. Sandstrom, H. Lundqvist, L. Einarsson, V. Tolmachev, Evaluation of [111/114mIn]CHX-A'-DTPAZHER2:342, an Affibody ligand conjugate for targeting of HER2-expressing malignant tumors, Q. J. Nucl. Med. Mol. Imaging 51 (2007) 314–323.
[24] M. Altai, Z. Varasteh, K. Andersson, A. Eek, O. Boerman, A. Orlova, In vivo and in vitro studies on renal uptake of radiolabeled affibody molecules for imaging

of HER2 expression in tumors, Cancer Biother. Radiopharm. 28 (2013) 187–195.
[25] A. Orlova, A. Jonsson, D. Rosik, H. Lundqvist, M. Lindborg, L. Abrahmsen, C. Ekblad, F.Y. Frejd, V. Tolmachev, Site-specific radiometal labeling and improved biodistribution using ABY-027, a novel HER2-targeting affibody molecule-albumin-binding domain fusion protein, J. Nucl. Med. 54 (2013) 961–968.
[26] V. Tolmachev, E. Mume, S. Sjöberg, F.Y. Frejd, A. Orlova, Influence of valency and labelling chemistry on in vivo targeting using radioiodinated HER2-binding Affibody molecules, Eur. J. Nucl. Med. Mol. Imaging 36 (2009) 692–701.
[27] G. Liu, D.J. Hnatowich, Labeling biomolecules with radiorhenium: a review of the bifunctional chelators, Anticancer Agents Med. Chem. 7 (2007) 367–377.
[28] S. Liu, Bifunctional coupling agents for radiolabeling of biomolecules and target-specific delivery of metallic radionuclides, Adv. Drug Deliv. Rev. 60 (2008) 1347–1370.
[29] C. Bolzati, D. Carta, N. Salvarese, F. Refosco, Chelating systems for (99m)Tc/(188)Re in the development of radiolabeled peptide pharmaceuticals, Anticancer Agents Med. Chem. 12 (2012) 428–461.
[30] T. Engfeldt, T. Tran, A. Orlova, C. Widström, J. Feldwisch, L. Abrahmsen, A. Wennborg, A.E. Karlström, V. Tolmachev, 99mTc-chelator engineering to improve tumour targeting properties of a HER2-specific Affibody molecule, Eur. J. Nucl. Med. Mol. Imaging 34 (2007) 1843–1853.
[31] T.A. Tran, T. Ekblad, A. Orlova, M. Sandström, J. Feldwisch, A. Wennborg, L. Abrahmsén, V. Tolmachev, A. Eriksson Karlström, Effects of lysine-containing mercaptoacetyl-based chelators on the biodistribution of 99mTc-labeled anti-HER2 Affibody molecules, Bioconjug. Chem. 19 (2008) 2568–2576.
[32] T. Ekblad, A. Orlova, J. Feldwisch, A. Wennborg, A. Eriksson Karlström, V. Tolmachev, Positioning of (99m)Tc-chelators influences radiolabeling, stability and biodistribution of Affibody molecules, Bioorg. Med. Chem. Lett. 19 (2009) 3912–3914.
[33] T.A. Tran, D. Rosik, L. Abrahmsén, M. Sandström, A. Sjöberg, H. Wållberg, S. Ahlgren, A. Orlova, V. Tolmachev, Design, synthesis and biological evaluation of a multifunctional HER2-specific Affibody molecule for molecular imaging, Eur. J. Nucl. Med. Mol. Imaging 36 (2009) 1864–1873.
[34] S. Ahlgren, H. Wållberg, T.A. Tran, C. Widström, M. Hjertman, L. Abrahmsén, D. Berndorff, L.M. Dinkelborg, J.E. Cyr, J. Feldwisch, A. Orlova, V. Tolmachev, Targeting of HER2-expressing tumors with a site-specifically 99mTc-labeled recombinant affibody molecule, ZHER2:2395, with C-terminally engineered cysteine, J. Nucl. Med. 50 (2009) 781–789.
[35] H. Wållberg, A. Orlova, M. Altai, S.J. Hosseinimehr, C. Widström, J. Malmberg, S. Ståhl, V. Tolmachev, Molecular design and optimization of 99mTc-labeled recombinant affibody molecules improves their biodistribution and imaging properties, J. Nucl. Med. 52 (2011) 461–469.
[36] M. Altai, H. Wållberg, A. Orlova, M. Rosestedt, S.J. Hosseinimehr, V. Tolmachev, S. Ståhl, Order of amino acids in C-terminal cysteine-containing peptide-based chelators influences cellular processing and biodistribution of 99mTc-labeled recombinant affibody molecules, Amino Acids 42 (2012) 1975–1985.
[37] T. Engfeldt, A. Orlova, T. Tran, A. Bruskin, C. Widström, A.E. Karlström, V. Tolmachev, Imaging of HER2-expressing tumours using a synthetic Affibody molecule containing the 99mTc-chelating mercaptoacetyl-glycyl-glycyl-glycyl (MAG3) sequence, Eur. J. Nucl. Med. Mol. Imaging 34 (2007) 722–733.
[38] T. Ekblad, T. Tran, A. Orlova, C. Widström, J. Feldwisch, L. Abrahmsén, A. Wennborg, A.E. Karlström, V. Tolmachev, Development and preclinical characterisation of 99mTc-labelled affibody molecules with reduced renal uptake, Eur. J. Nucl. Med. Mol. Imaging 35 (2008) 2245–2255.
[39] U. Seitz, B. Neumaier, G. Glatting, J. Kotzerke, D. Bunjes, S.N. Reske, Preparation and evaluation of the rhenium-188-labelled anti-NCA antigen monoclonal antibody BW 250/183 for radioimmunotherapy of leukaemia, Eur. J. Nucl. Med. 26 (1999) 265–1273.
[40] D. Bunjes, I. Buchmann, C. Duncker, U. Seitz, J. Kotzerke, M. Wiesneth, D. Dohr, M. Stefanic, A. Buck, S.V. Harsdorf, G. Glatting, W. Grimminger, T. Karakas, G. Munzert, H. Döhner, L. Bergmann, S.N. Reske, Rhenium 188-labeled anti-CD66 monoclonal antibody to intensify the conditioning regimen prior to stem cell transplantation for patients with high-risk acute myeloid leukemia or myelodysplastic syndrome: results of a phase I–II study, Blood 98 (2001) 565–572.
[41] J.E. Cyr, D.A. Pearson, D.M. Wilson, C.A. Nelson, M. Guaraldi, M.T. Azure, J. Lister-James, L.M. Dinkelborg, R.T. Dean, Somatostatin receptor-binding peptides suitable for tumor radiotherapy with Re-188 or Re-186. Chemistry and initial biological studies, J. Med. Chem. 50 (2007) 1354–1364.
[42] Y.B. Miao, N.K. Owen, D. Whitener, F. Gallazzi, T.J. Hoffman, T.P. Quinn, In vivo evaluation of 188Re-labeled alpha-melanocyte stimulating hormone peptide analogs for melanoma therapy, Int. J. Cancer 101 (2002) 480–487.
[43] G. Liu, J. He, S. Dou, S. Gupta, J.L. Vanderheyden, M. Rusckowski, D.J. Hnatowich, Pretargeting in tumored mice with radiolabeled morpholino oligomer showing low kidney uptake, Eur. J. Nucl. Med. Mol. Imaging 31 (2004) 417–424.
[44] H. Karacay, W.J. McBride, G.L. Griffiths, R.M. Sharkey, J. Barbet, H.J. Hansen, D.M. Goldenberg, Experimental pretargeting studies of cancer with a humanized anti-CEA x murine anti-[In-DTPA] bispecific antibody construct and a (99m)Tc-/(188)Re-labeled peptide, Bioconjug. Chem. 11 (2000) 842–854.
[45] A. Orlova, T.A. Tran, T. Ekblad, A.E. Karlström, V. Tolmachev, (186)Re-maSGS-Z (HER2:342), a potential Affibody conjugate for systemic therapy of HER2-expressing tumours, Eur. J. Nucl. Med. Mol. Imaging 37 (2010) 260–269.
[46] H. Wållberg, P.Å. Löfdal, K. Tschapalda, Affinity recovery of eight HER2-binding affibody variants using an anti-idiotypic affibody molecule as capture ligand, Protein Expr. Purif. 76 (2011) 127–135.
[47] H. Björkelund, L. Gedda, P. Barta, M. Malmqvist, K. Andersson, Gefitinib induces epidermal growth factor receptor dimers which alters the interaction characteristics with ^{125}I-EGF, PLoS One 6 (2011) e24739.
[48] A. Orlova, V. Tolmachev, R. Pehrson, M. Lindborg, T. Tran, M. Sandström, F.Y. Nilsson, A. Wennborg, L. Abrahmsén, J. Feldwisch, Synthetic Affibody molecules: a novel class of affinity ligands for molecular imaging of HER2 expressing malignant tumors, Cancer Res. 67 (2007) 2178–2189.
[49] G.W. Visser, M. Gerretsen, J.D. Herscheid, G.B. Snow, G. van Dongen, Labeling of monoclonal antibodies with rhenium-186 using the MAG3 chelate for radioimmunotherapy of cancer: a technical protocol, J. Nucl. Med. 34 (1993) 1953–1963.
[50] A.H. Brouwers, J.E. van Eerd, C. Frielink, E. Oosterwijk, W.J. Oyen, F.H. Corstens, O.C. Boerman, Optimization of radioimmunotherapy of renal cell carcinoma: labeling of monoclonal antibody cG250 with 131I, 90Y, 177Lu, or 186Re, J. Nucl. Med. 45 (2004) 327–337.
[51] S. Kinuya, K. Yokoyama, K. Kobayashi, S. Motoishi, K. Onoma, N. Watanabe, N. Shuke, H. Bunko, T. Michigishi, N. Tonami, Experimental radioimmunotherapy with 186Re-MAG3-A7 anti-colorectal cancer monoclonal antibody: comparison with 131I-counterpart, Ann. Nucl. Med. 15 (2001) 199–202.
[52] M.J. Koppe, R.P. Bleichrodt, A.C. Soede, A.A. Verhofstad, D.M. Goldenberg, W.J. Oyen, O.C. Boerman, Biodistribution and therapeutic efficacy of 125/131I-, 186Re-, 88/90Y-, or 177Lu-labeled monoclonal antibody MN-14 to carcinoembryonic antigen in mice with small peritoneal metastases of colorectal origin, J. Nucl. Med. 45 (2004) 1224–1232.
[53] S. Ahlgren, K. Andersson, V. Tolmachev, Kit formulation for 99mTc-labeling of recombinant anti-HER2 Affibody molecules with a C-terminally engineered cysteine, Nucl. Med. Biol. 37 (2010) 539–549.
[54] A. Orlova, H. Wållberg, S. Stone-Elander, V. Tolmachev, On the selection of a tracer for PET imaging of HER2-expressing tumors: direct comparison of a 124I-labeled affibody molecule and trastuzumab in a murine xenograft model, J. Nucl. Med. 50 (2009) 417–425.
[55] L.S. Zuckier, O. Dohan, Y. Li, C. Chang, N. Carrasco, E. Dadachova, Kinetics of perrhenate uptake and comparative biodistribution of perrhenate, pertechnetate, and iodide by NaI symporter-expressing tissues in vivo, J. Nucl. Med. 45 (2004) 500–507.